Adsorption of Water and Methanol on Silica Hydroxyls: Ab Initio Energy and Frequency Calculations

A. G. Pelmenschikov,*,† G. Morosi, and A. Gamba

Dipartimento di Chimica Fisica ed Elettrochimica, Universitá di Milano−Sede di Como, Via Lucini 3, 22100 Como, Italy

Received: October 9, 1996[⊗]

Two hypothetical mechanisms proposed in the literature for the coordination of H_2O and CH_3OH on the isolated silica OH group are reexamined by computations on the related molecular models at SCF, MP2, and DFT levels. The computed energies suggest that these molecules stabilize on the isolated OH group by means of two hydrogen bonds, acting as a proton acceptor toward the silica OH group and as a proton donor toward a nearby SiOSi bridge. The alternative surface structures, with H_2O and CH_3OH acting exclusively as a proton acceptor toward the isolated OH group, are found to be less stable by ∼8 kJ/mol. The check of these mechanisms against experimental IR data using the computed frequency shifts of CH_3OH upon the adsorption supports these results. The ab initio calculations suggest no significant difference in mechanism between the adsorptions on the isolated and geminal OH groups of silica. When stabilizing on a geminal OH group, H_2O and CH_3OH can form the extra hydrogen bond not only with the nearby SiOSi bridge but also with the complementary geminal OH group.

Introduction

The mechanism of interaction between water and the isolated OH group of silica is a debated theoretical problem. Two alternatives are proposed for this mechanism on the basis of ab initio energy calculations on molecular models.[1−9] The first one, with H_2O acting toward the OH group as a proton acceptor (structure **1**), was suggested in refs 1−8. In those studies

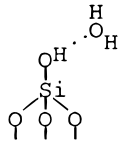

1

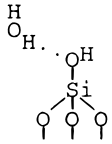

2

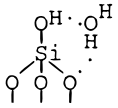

3

structure **1** was shown to be significantly more stable than structure **2**, the H_2O bonded to the OH group as a proton donor. The most sophisticated energy analysis of these two structures was performed by Ugliengo et al.[7,8] at the MP2/TZ++(2d,2p)//SCF/DZP level using H_3SiOH as a molecular model of the isolated OH group. The second mechanism was suggested in our investigation[9] at the SCF/6-31G(d) and MP2/6-31G(d,p)//SCF/6-31G(d) levels with the $Si(OH)_4$ model of the surface. In this mechanism H_2O acts both as a proton acceptor and as a proton donor simultaneously toward the OSiOH surface site including the isolated OH group and a nearby O atom (structure **3**). Moreover, our calculations showed structure **1** to be unstable: its optimization, allowing the O−H···O angle to vary, turns structure **1** into structure **3** without an energy barrier.

Also, for the interaction of methanol with the isolated silica OH group, Ugliengo et al.[8,10] supposed the adsorbed molecule to behave exclusively as a proton acceptor (structure **4**). By analogy with their calculations of H_2O on the isolated OH group,[7,8] they used the $HOSiH_3$ model of the surface which enabled only one alternative structure to be considered, namely

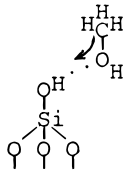

4

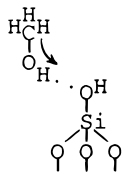

5

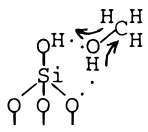

6

structure **5**. This structure was found to be substantially less stable than structure **4**.[10] The calculations were done at the SCF level with the 6-31G(d,p) and DZP (TZP on O atoms) basis sets. We studied this reaction at the SCF/6-31G(d) and SCF/3-21G levels using the $CH_3OH{\cdot}Si(OH)_4$ model,[11,12] which allowed us to examine not only structures **4** and **5** but also structure **6**. Like for the H_2O adsorption, our results suggested the 2-fold H-bonded species (structure **6**) to be the most energetically preferable.

In our studies[11,12] we proposed to use also the computed $\Delta\nu(CH_3)$ frequency shifts of CH_3OH upon the adsorption for discriminating between the alternative mechanisms. We showed that in H-bonding interactions the $\Delta\nu(CH_3)$ shifts of the CH_3O-containing molecules depend on the electron charge shift on the CH_3 group: an electron charge shift which decreases/increases the C^+-H^- polarity of the C−H bonds makes the $\nu(CH_3)$ frequencies shift to higher/lower wavenumbers due to the increase/decrease of the covalent contributions to the C−H bonds. This electron mechanism agrees with the second Gutmann's rule[13] and the Chung−Bennett empirical dependence.[14] Therefore structure **4** proposed by Ugliengo et al.[8,10] contradicts the experimental fact that the CH_3OH adsorption on the silica OH groups causes the $\nu(CH_3)$ to decrease.[15−18] In this structure the withdrawal of the electron charge from the CH_3 group should increase the $\nu(CH_3)$ frequencies[11,12] (the directions of electron charge transfer are indicated by arrows in the structures). For instance, in the similar interactions of CH_3OCH_3 with the silica and zeolitic OH groups (structures **7** and **8**), the $\nu_{as}(CH_3)$, $\nu''_{as}(CH_3)$, and $\nu_s(CH_3)$ frequencies increase by 9, 21, 11 and 23, 51, 24 cm^{-1}, respectively.[17,18] As to structure **6**, its computed $\Delta\nu(CH_3)$ frequency shifts were found to be in good agreement with the IR data.[11,12]

† Present address: Universitá di Milano−Sede di Como, Via Lucini 3, 22100 Como, Italy.

⊗ Abstract published in *Advance ACS Abstracts,* January 1, 1997.

S1089-5639(96)03105-2 CCC: $14.00

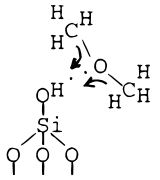

7

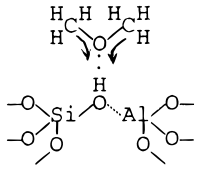

8

As an additional support of the 2-fold hydrogen-bonded H_2O and CH_3OH species on the OSiOH silica site, we note that they conform to the well-known bifunctionality of water and methanol,[19−22] which leads these molecules to form similar cyclic hydrogen-bonded complexes

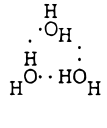

9

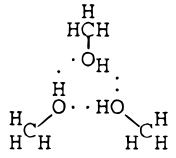

10

in solution. In these complexes the energy gain due to the extra hydrogen bonding and the cooperative effect offset the energy loss for the strong deviation of the OH···O fragments from linearity.[22]

Recently, Sauer et al.[8] reported BSSE corrected SCF/MINI-1 and MP2//SCF/DZP energy calculations of the closed and open H_2O species using $HOSiH_2OSiH_3$ as a molecular model of the OSiOH silica site, the nearby SiOSi bridge being mimicked by the $SiOSiH_3$ group. They found that there is no extra hydrogen bonding of H_2O on the isolated OH group: the H_2O experiences only a nonspecific interaction with the siloxane bridge, the smallest R_{OH} distance between the H_2O and SiOSi being larger than the sum of the H and O van der Waals radii (2.6 Å). The opposite result of our calculations[9] was suggested to be biased by the $Si(OH)_4$ model of the (Si)OSiOH site: in their opinion the SiOH moiety is not adequate for mimicking the SiOSi bridge in the discussed interaction. These calculations reinforced their previous theoretical inference about the 1-fold hydrogen bonding of H_2O and CH_3OH on the isolated OH group.[1−4,7,8,10] The fact that this mechanism disagrees with the experimental IR data on the CH_3OH adsorption on silica[11,12,17] was not taken into account in this study.

To get consistent theoretical results on energy and frequencies for H_2O and CH_3OH interacting with the isolated OH group of silica, in the present study we reexamine the above-mentioned adsorption structures employing more extended molecular models and more accurate quantum chemical approximations compared to those adopted in the previous theoretical studies on this subject.[1−12,17] As the contradictory findings on the relative stabilities of the cyclic and open structures resulted from ab initio calculations on molecular models of different size,[8−12] we check the model size effect on the calculated adsorption energies. On the basis of the current view[10,23] of the prevailing electrostatic nature of the moderate strength H-bonding, we also perform an analysis of the Coulombic interactions between the H-bonded partners in the studied molecular models in order to interpret the results of the ab initio energy calculations. When identifying the adsorption structures of methanol using experimental IR data, the observed $\Delta\nu$(OH) and $\Delta\delta$(OH) shifts of methanol on the SiOH groups are considered for the first time besides the $\Delta\nu(CH_3)$ shifts.[11,12,17] We also touch upon the problem of the H_2O and CH_3OH adsorption on the geminal silica OH group.[24]

Although results of energy and frequency calculations are complementary in our study, we believe that the frequency analysis provides the main proof for the proposed adsorption mechanism. As the frequency shifts of adsorbed molecules depend in unique fashion on the adsorption mechanism, experimental IR data can be very useful for discriminating among the alternative structures for which energy calculations lead to contradictory results. Another important point is that according to our results[25,26] the computed frequency shifts of simple probe molecules on oxides are significantly less sensitive to the model size and basis set effects than the computed binding energies. Moreover, in many cases, using well-established empirical dependencies of the frequency shifts of probe molecules on adsorption mechanism, a hypothetical structure can be supported or unambiguously ruled out on the basis of a simple qualitative analysis of experimental IR data.

Details of Calculations and Frequency Analysis

Ab initio calculations were performed with the GAUSSIAN-92 and GAUSSIAN-94 packages.[27,28] Various approximations were used, depending on the desired accuracy. For convenience their specifications are given below when discussing particular problems. Corrections to the adsorption energies for the basis set superposition error (BSSE) were estimated by the counterpoise method.[29] Electrostatic potential energy derived net charges (PED) were computed at SCF level by means of the GAUSSIAN-94 POP=CHELPG option which utilizes the Breneman−Wiberg approximation.[30] Corrections to SCF molecular electrostatic potentials due to the electron correlation are usually insignificant.[10,23]

For checking hypothetical CH_3OH surface species against experimental IR data, we used their computed $\Delta\nu'_{as}(CH_3)$, $\Delta\nu_s(CH_3)$, $\Delta\nu$(OH), and $\Delta\delta$(OH) shifts. The calculated $\Delta\nu''_{as}(CH_3)$ shifts were not involved in our theoretical analysis, as the harmonic frequency approximation does not take into account the Fermi resonances of the $\nu''_{as}(CH_3)$ mode with the overtones and combinations of the $\delta(CH_3)$ modes.[31,32] Moreover, a conclusive experimental assignment of the $\nu''_{as}(CH_3)$ band of CH_3OH on the OH silica groups has been missing in the literature up to now.[17]

When discussing the CH_3OH adsorption, we use the computed proton donor OH frequency shifts for a qualitative analysis only. Results of a recent theoretical analysis[33] of the different contributions to the OH frequency shifts of water, methanol, and silanol dimers suggest that both the harmonic frequency approximation and the level of the ab initio treatment adopted in our study are not sufficient for a quantitative description of the proton donor OH frequency shifts (see also ref 34). Moreover, the quantitative prediction of these shifts for the case of the CH_3OH adsorption would be useless for identifying the discussed H-bonded species as their precise experimental values are unknown. As Borello et al.[15,16] showed (see also below), the CH_3OH adsorption produces a very broad, complex OH stretching band in the 3600−3200 cm^{-1} region, and it is impossible to distinguish all the subbands owing to their large width and strong overlap. The same sort of experimental difficulties have led to a significant discrepancy in the assignment of the H_2O and SiOH $\Delta\nu$(OH) shifts for the case of the H_2O adsorption on silica (see refs 7 and 8 and references therein). Therefore we also do not use the computed OH frequency shifts of the adsorbed H_2O for discriminating between the alternative mechanisms.

In analyzing experimental IR data, we consider the IR bands of methanol on silica hydroxyls to be produced mainly by CH_3OH species on the isolated OH groups, the concentration of

TABLE 1: BSSE Corrected Binding Energies of Closed, E^c, and Open, E^o, H_2O and CH_3OH Adsorption Structures[a] (kJ/mol)

	6-31G(d)		MP2/6-31G(d)		BLYP/CBS1	
	E^c	E^o	E^c	E^o	E^c	E^o
1a, **1b**	29 (36)	28 (33)	36 (52)	35 (45)	24 (40)	21 (37)
2a, **2b**	28 (35)	21 (26)	38 (54)	28 (38)	35 (51)	23 (39)
3a, **3b**			38 (56)	26 (37)	34 (50)	24 (35)
4a, **4b**			39 (54)	30 (40)	36 (53)	24 (40)
5a, **5b**			39 (55)	32 (43)	36 (51)	28 (40)

[a] $E^c(E^o) = E$(complex) − [E(substrate) + E(adsorbate)]. Numbers in parentheses are BSSE uncorrected values.

the geminal OH groups being smaller than that of the isolated ones by a factor of at least 3 (ref 8 and references therein).

For all the examined models of the H_2O and CH_3OH adsorption, our calculation results show only one energy minimum corresponding to the 2-fold H-bonding mechanism. The calculations of the constrained 1-fold H-bonded structures are performed mainly for examining whether the energy preference of the closed to open structures is large enough for the extra H-bond to play a significant role in the adsorption. As mentioned in the Introduction this problem emerges from conflicting situation in interpreting the reaction mechanism by different authors, which is mainly caused by the choice of different models for silica hydroxyls. Therefore these results are also used to check the adequacy of these models, which is important for their further employment in studying the adsorption on silica.

In the figures, of all the optimized geometry parameters, only the H-bond lengths are reported, computed at MP2 level. The difference between the H-bond lengths predicted by the MP2 and DFT calculations is insignificant. For the models involved in the electrostatic energy analysis, the SCF H-bond lengths and OH···O bond angle including the H_2O OH group are also reported.

Results and Discussion

1. Energy Analysis. *1.1 Ab Initio Calculations*. In Table 1 we report the BSSE corrected MP2/6-31G(d) binding energies of H_2O on the OSiOH site computed with

(a) the $H_2O{\cdot}HOSiH_2OSiH_3$ model (**1a** and **1b**, Figure 1) used by Sauer et al.,[8] some O atoms in the first coordination spheres of the Si atoms being mimicked by H atoms;

(b) the $H_2O{\cdot}(HO)_3SiOSi(OH)_3$ model (**2a** and **2b**, Figure 1) with the "natural" nearest surrounding of the Si atoms. In these models the SiOSi angle was fixed to 140°, the averaged value for silica. The OSiO, OSiH, and HSiH angles were kept equal to 109.5°. Models **1a** and **2a** of the closed H_2O structure were optimized under the C_s symmetry constraint. Models **1b** and **2b** of the open H_2O structure were optimized with the additional ∠O−H···O = 180° and ∠H···O−X = 123° geometry constraints allowing the formation of only one H-bond: these values correspond to the optimal ones for the 1-fold H-bonding.[6,35]

The energy preference $E^c - E^o = 1$ kJ/mol of the closed to open structure computed with the $H_2O{\cdot}HOSiH_2OSiH_3$ model is too small for a definitive discrimination between the two examined mechanisms. As we will show below, the zero-point and thermal corrections should cancel out this small difference in the binding energy. Thus, in agreement with the theoretical study by Sauer et al.,[8] the $H_2O{\cdot}HOSiH_2OSiH_3$ model suggests that a nearby siloxane bridge does not play a significant role in stabilizing water complexes on the terminal OH groups. As to the extended $H_2O{\cdot}(HO)_3SiOSi(OH)_3$ model, the corresponding $E^c - E^0 = 10$ kJ/mol value implies the 2-fold H-bonding

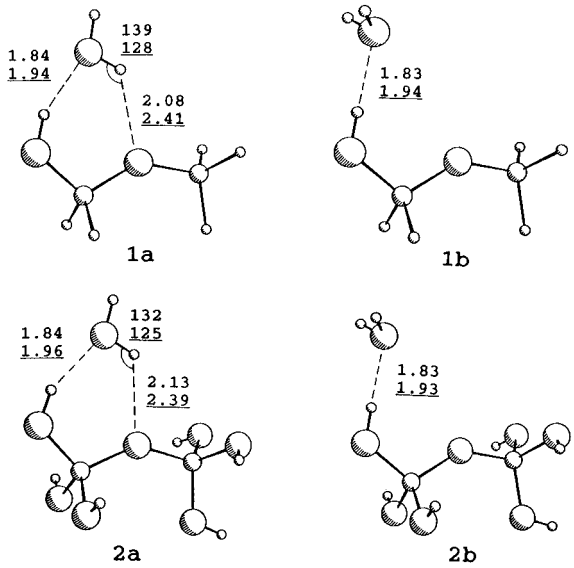

Figure 1. Molecular models of water on the OSiOH site of silica. H-bond lengths in angstroms, bond angles in degrees at the MP2/6-31G(d) and SCF/6-31G(d) (underlined) levels.

mechanism of the adsorption. We computed these models also by a DFT method using the GAUSSIAN-94 BLYP option, which combines the exchange functional of Becke[36] with the correlation functional of Lee, Yang, and Parr.[37] These calculations were performed with a larger, combined basis set (CBS1): the 6-311G(d,p) basis set for H_2O, the adsorbing H atom, and the O atoms surrounding the Si atom bonded to the adsorbing OH group and the 6-31G(d) basis set for the rest of the models. The BLYP/CBS1 calculations reinforce the MP2/6-31G(d) results (Table 1). According to the generally accepted methodology of the molecular approach, among the two examined models $H_2O{\cdot}(HO)_3SiOSi(OH)_3$ has to be taken as the most reliable one, the $H_2O{\cdot}HOSiH_2OSiH_3$ model being obtained by its simplification. Therefore these results suggest that the $H_2O{\cdot}HOSiH_2OSiH_3$ model used by Sauer et al.[8] is inadequate for studying the mechanism in question. The reason of this inadequacy is explained below by the analysis of the Coulombic interactions in these models.

To check whether the neglect of the surrounding lattice in the $(HO)_3SiOSi(OH)_3$ surface model can significantly influence the result, we examined the convergence of the extra stabilization energy at the SCF/6-31G(d) level upon increasing the

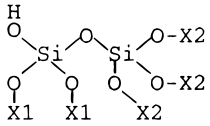

model size in the series (X1 = X2 = H) < (X1 = $Si(OH)_3$, X2 = H) < (X1 = H, X2 = $Si(OH)_3$) < (X1 = X2 = $Si(OH)_3$). Our calculations for the **1a**, **1b**, **2a**, and **2b** models (Table 1) suggest that in computing the binding energy the SCF/6-31G(d) and BSSE corrected MP2/6-31G(d) methods lead to nearly the same results: the MP2 and BSSE corrections to the E^c and E^o energies on going from the SCF/6-31G(d) to BSSE corrected MP2/6-31G(d) approximation about compensate each other. Such mutual compensation of the MP2 and BSSE corrections takes place also for the binding energies of $2CH_3OH$, $CH_3OH{\cdot}SiH_3OH$, and $2SiH_3OH$ complexes computed with a DZP (TZP on oxygen) basis set.[10] The models with X1 = $Si(OH)_3$ and X2 = H or $Si(OH)_3$ were computed without geometry optimization, the geometry of the $H_2O{\cdot}HOSiO_2SiO_3$ fragments of the closed and open structures being equal to those optimized for

TABLE 2: SCF/6-31G(d) Binding Energies of Closed, E^c, and Open, E^o, Adsorption Structures of Water[a] (kJ/mol)

$HOSi(OX1)_2OSi(OX2)_3$			
X1	X2	E^c	E^o
H	H	35	26
$Si(OH)_3$	H	31	22
H	$Si(OH)_3$	36	24
$Si(OH)_3$	$Si(OH)_3$	33	22

[a] $E^c(E^o) = E$(complex) − [E(substrate) + E(adsorbate)].

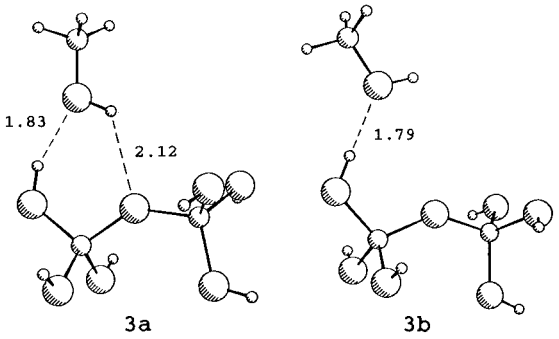

Figure 2. Molecular models of methanol on the OSiOH site of silica. H-bond lengths in angstroms at the MP2/6-31G(d) level.

2a and **2b** (Figure 1). The SCF/6-31G(d) calculations show that the increase of the model size does not effect the $E^c - E^o \simeq 10$ kJ/mol energy preference of the closed to open structure (Table 2). This result supports the adequacy of the $(HO)_3SiOSi(OH)_3$ model of the (Si)OSiOH site for studying the extra stabilization effect.

Also for CH_3OH on the OSiOH site our MP2/6-31G(d) and BLYP/CBS1 calculations using the $(HO)_3SiOSi(OH)_3$ model (Figure 2) lead to a similar result: the closed CH_3OH structure (**3a**) is more stable than the open one (**3b**) by ∼10 kJ/mol (Table 1). This reflects the closeness of the acid−base properties of H_2O and CH_3OH, which led us to suppose that these molecules interact with the isolated SiOH silica group by the same mechanism and involve both of them in the study of this mechanism.[9,11,12,17]

We also computed the energy gain on going from the open to closed structure for the case of the H_2O and CH_3OH adsorption on the geminal silica OH groups, the adsorbed molecule forming the extra H-bond toward the neighboring OH group. The calculations were performed at the MP2/6-31G(d) and BLYP/CBS1 levels with the $Si(OH)_4$ model of the geminal OH groups (Figure 3). Similar to the $(HO)_3SiOSi(OH)_3$ model of the (Si)OSiOH site, this model of the (H)OSiOH site includes only the first coordination sphere of silicon atoms with respect to the surface OH groups. Our calculations suggest that for the same configuration of the (Si)OSiOH (**2a**, **2b**, **3a**, and **3b**) and (H)OSiOH (**4a**, **4b**, **5a**, and **5b**) sites the difference in energy between the extra H-bonds toward the complementary geminal OH group and toward the nearby siloxane bridge is insignificant (Table 1). This result also justifies the use of the $Si(OH)_4$ model for simulating the H_2O and CH_3OH adsorption on the (Si)-OSiOH site in our previous studies.[9,11,12,17]

As the found difference of ∼10 kJ/mol in binding energy between the open and closed structures is quite small, the zero-point and thermal corrections should be taken into account when discussing their relative stability. However, the geometry constraints imposed on the above-discussed models do not allow one to employ them for evaluating all the relevant vibrational frequencies. Therefore we used the fully optimized M·$Si(OH)_4$ and M·$HOSiH_3$ (M = H_2O, CH_3OH) MP2/6-31G(d) models (Figure 4) to examine the effect of these corrections for the

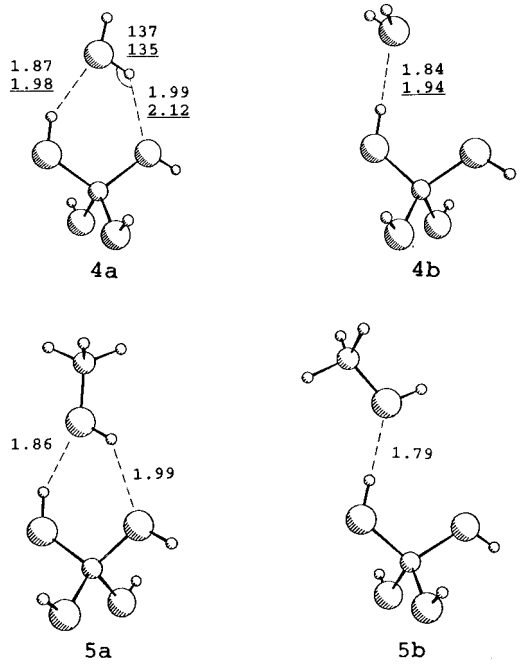

Figure 3. Molecular models of water and methanol on geminal OH groups of silica. H-bond lengths in angstroms, bond angles in degrees at the MP2/6-31G(d) and SCF/6-31G(d) (underlined) levels.

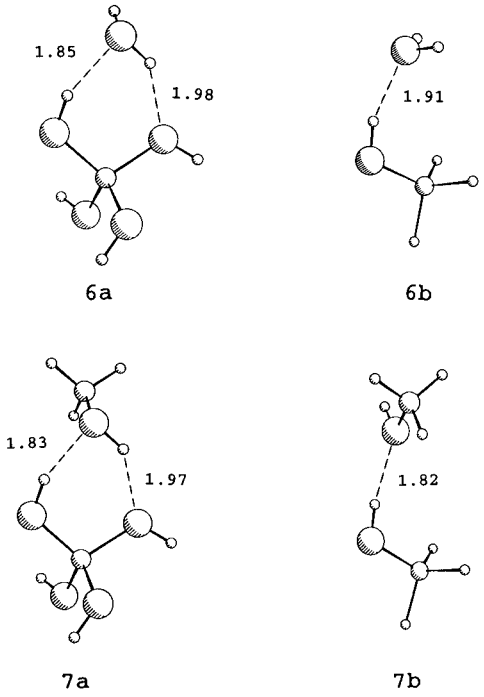

Figure 4. M·$Si(OH)_4$ and M·$HOSiH_3$ (M = H_2O and CH_3OH) complexes fully optimized at the MP2/6-31G(d) level. H-bond lengths in angstroms.

2-fold and 1-fold H-bonding mechanisms, respectively. According to the results of the extensive use of $HOSiH_3$ as a model of the isolated silica OH group,[7,8,10,23,24] this model is adequate for the quantitative description of the 1-fold H-bonding interactions on silica hydroxyls. The M·$HOSiH_3$ normal mode which corresponds to the M torsion around the H-bond was treated as a free rotation, contributing $0.5RT$ to the enthalpy.[38] The results of our calculations (Table 3) show that the zero-point (ΔZPE) and thermal (ΔH_{th}) corrections to the frozen nuclei binding energies can decrease the difference in stability between the closed (**6a** and **7a**) and open (**6b** and **7b**) structures by ∼2.5 kJ/mol. This effect is mainly accounted for by the inter-

TABLE 3: Adsorption Energy ($-\Delta E$), Zero-Point (ΔZPE), and Thermal (ΔH_{th}) Corrections and Standard Heat of Formation ($\Delta H°$)[a] (kJ/mol)

model	$-\Delta E$	ΔZPE	ΔH_{th}	$\Delta H°$
6a	−35.7 (−55.9)	12.5	−3.3	−26.5
6b	−24.7 (−39.4)	8.2	−1.3	−17.8
7a	−35.5 (−57.8)	9.5	−0.8	−26.8
7b	−28.4 (−40.7)	6.4	−0.3	−22.3

[a] MP2/6-31G(d). Numbers in parentheses are not BSSE corrected values.

TABLE 4: Electrostatic Contributions to the Extra Stabilization Effect on Going from Open to Closed Structure[a] (kJ/mol)

	$H_2O\cdot HOSiH_2OSiH_3$	$H_2O\cdot (HO)_3SiOSi(OH)_3$	$H_2O\cdot Si(OH)_4$
O1H1	−6	−6	−5
Si1	−8	−27	1
O2	−21	−20	−50
other atoms	16	17	17
total	−19	−36	−37

[a] PED charges and geometries are derived from SCF/6-31G(d) **1a**, **1b**, **2a**, **2b**, **4a**, and **4b** models.

molecular vibrational frequencies of $M\cdot Si(OH)_4$ being larger than those of $M\cdot HOSiH_3$, which results from the extra H-bond in $M\cdot Si(OH)_4$ and makes its ΔZPE be larger (Table 3). To summarize, these results suggest that the total effect of the zero-point and thermal corrections on the relative stability of the closed and open structures is not essential.

It is to be noted that the difference in the MP2/6-31G(d) adsorption energy between the fully optimized closed and open H_2O (**6a** and **6b**) and CH_3OH (**7a** and **7b**) structures closely corresponds to that between the related constrained models (**4a**, **4b**, **5a**, and **5b**) (cf. Tables 1 and 3). This fact warrants our use of the constrained models for estimating the relative stability of the 2-fold and 1-fold H-bonded species.

1.2. Electrostatic Interaction Analysis. Ugliengo et al. showed[23] that the pure electrostatic interaction plays the predominant role in the moderate strength H-bonding. As a consequence, the successful use of small molecular models for describing the H-bonding on oxides[8] implies that an H-bonding mechanism on an oxide should be mainly defined by the electrostatic interaction of the adsorbed molecule with "the site", i.e. a very few nearby surface atoms. Therefore, below we interpret the difference in the extra stabilization energy between the $H_2O\cdot HOSiH_2OSiH_3$ model used by Sauer et al.[8] and the extended $H_2O\cdot(HO)_3SiOSi(OH)_3$ model in terms of the difference in the electrostatic properties between the OSiOH adsorbing sites of these models.

In Table 4 we compare the electrostatic contributions to the H_2O extra stabilization energy from the atoms of the OSiOH site of the $HOSiH_2OSiH_3$ and $(HO)_3SiOSi(OH)_3$ models. The calculations were performed using the geometry and PED charges (Table 5) of the optimized **1a**, **1b**, **2a**, and **2b** SCF/6-31G(d) models. The numbering of the atoms of the $HOSiH_2OSiH_3$ and $(HO)_3SiOSi(OH)_3$ models is shown in the following schemes

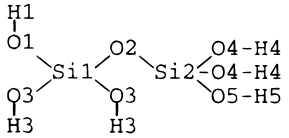

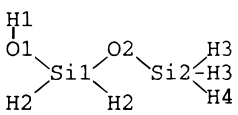

The data of Table 4 suggest that the difference in the extra stabilization energy between these models is mainly accounted for by the difference in the electrostatic interaction of the adsorbed H_2O molecule with the Si atom of the OSiOH site, the contributions to the extra stabilization from the adsorbing OH group, the bridging O atom, and the rest of the models being approximately equal. As follows from the data of Table 5, this effect results from the significant underestimation (by ~0.5 au) of the corresponding q(Si) charge in the $HOSiH_2OSiH_3$ model compared to that in the extended $(HO)_3SiOSi(OH)_3$ model. This underestimation is explained by the not realistic chemical surroundings of the Si atom in the $HOSiH_2OSiH_3$ model, with the two nearby O atoms being mimicked by H atoms. The data of Table 4 also suggest that the stabilization effect cannot be simply interpreted in terms of the additional H-bonding to the O atom of the SiOSi bridge: a significant contribution to the extra stabilization energy is due to the H_2O electrostatic interaction with the nearest Si atom. This result further stresses the importance of the correct description of the q(Si) charge of the OSiOH site in studying the discussed mechanism.

TABLE 5: PED Charges[a] (au)

$H_2O\cdot HOSiH_2OSiH_3$			$H_2O\cdot(HO)_3SiOSi(OH)_3$			$H_2O\cdot Si(OH)_4$		
atom	**1a**	**1b**	atom	**2a**	**2b**	atom	**4a**	**4b**
H1	0.52	0.49	H1	0.58	0.52	H1	0.53	0.50
O1	−0.84	−0.87	O1	−0.98	−0.99	O1	−0.89	−0.93
Si1	1.17	1.23	Si1	1.68	1.72	Si1	1.58	1.63
O2	−0.66	−0.65	O2	−0.92	−0.89	O2	−0.94	−0.91
Si2	0.90	0.87	Si2	1.59	1.54			
H2	−0.23	−0.20	H3	0.42	0.43	H2	0.48	0.45
H3	−0.19	−0.16	O3	−0.79	−0.81	O3	−0.80	−0.82
H4	−0.21	−0.17	H4	0.44	0.44	H3	0.43	0.43
			O4	−0.81	−0.80			
			H5	0.47	0.47			
			O5	−0.92	−0.92			

[a] Derived from **1a**, **1b**, **2a**, **2b**, **4a**, and **4b** SCF/6-31G(d) models.

To check the cluster size effect on the electron distribution on the adsorption site, we examined the Mulliken atomic charges of the OSiOH site in the series of the SCF/6-31G(d) HOSi(OX1)OSi(OX2) (X1 = H, $Si(OH)_3$ and X2 = H, $Si(OH)_3$) models. In agreement with the suggestion by Ugliengo et al.,[23] we assumed that for a molecular fragment in a family of alike systems Mulliken populations should give a rough description of electronic flows. The averaged absolute change of the OSiOH atomic charges is ~0.02 au only, which conforms to the insignificant change of the SCF/6-31G(d) binding energies of H_2O on the OSiOH site in this series (see above).

In Table 4 we also report the electrostatic contributions to the extra stabilization energy for the case of the H_2O adsorption on the geminal OH groups. The calculations were performed with the geometry and PED charges (Table 5) of the **4a** and **4b** SCF/6-31G(d) models, the numbering of the atoms of the $Si(OH)_4$ model corresponding to the scheme

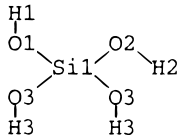

The comparison of the related contributions for the H_2O on the (Si)OSiOH and (H)OSiOH sites reveals a difference in the extra stabilization mechanism between these structures. As distinct from the H_2O adsorption on the (Si)OSiOH site, in the adsorption on the (H)OSiOH site the stabilization effect is mainly caused by the H_2O interaction with the O atom of the neighboring OH group, while the contribution from the Si atom is negligible. Also the difference in the geometry of the examined models conforms to this result (cf. the SCF/6-31G-

(d) geometry of **2a** and **4a**, Figures 1 and 3). In comparison with the (Si)OSiOH site, on the (H)OSiOH site the extra H-bond is shorter by ∼0.2 Å and the OHO angle of the OHncd··O fragment including this bond is closer to the optimal ∼180° value by ∼10°. Both these differences in geometry strengthen the extra H-bond but nearly eliminate the extra stabilization effect from the Si atom for the H_2O on the (H)OSiOH site. As a result, in spite of the difference in the electrostatic potential between the (Si)OSiOH and (H)OSiOH sites which causes the above-mentioned difference in geometry, the total extra stabilization effect on both the sites is approximately the same. Our analysis of the Coulombic interactions in the SCF/6-31G(d) **3a**, **3b**, **5a**, and **5b** models shows similar peculiarities for the mechanisms of the CH_3OH stabilization on these sites. The found difference between the 2-fold H-bonded species on the isolated and on the geminal OH hydroxyls agrees with the suggestion by Ugliengo et al.[24] that the SiOSi oxygen should be less basic than that of the SiOH group.

According to our results, the main features of the studied mechanism are accounted for by the interaction of the adsorbed molecules with the very small group of nearby surface atoms, i.e. with the adsorbing site. This fact further supports the basic assumption of the molecular approach to the modeling of the adsorption on oxides. At the same time, considering the long-range character of the Coulombic interactions, the contribution to the binding energy from the rest of the models is not negligible (Table 3). This means that in the real system, due to the heterogeneity of silica surface, the contribution from the rest of the surface should cause some variation of the binding energy but should not change the general adsorption mechanism defined by the site. The small change of the $HOSi(OX1)_2OSi(OX2)_3$ binding energy in the series (X1 = X2 = H) < (X1 = $Si(OH)_3$, X2 = H) < (X1 = H, X2 = $Si(OH)_3$) < (X1 = X2 = $Si(OH)_3$) supports this suggestion (Table 2).

PED models can provide only a rough description of the adsorption interactions.[23] Even considering the fact that H-bonding is basically related to electrostatic interactions,[10,23] the simulation of the electron density of molecules by simple monopoles centered on nuclei position is rather crude. However, in agreement with a conclusion by Ugliengo et al.,[23] our results suggest that for closely related complexes the errors are very systematic. Therefore, although the PED models overestimate the extra stabilization energy by ∼−20 kJ/mol compared with the ab initio models (cf. Tables 1 and 4), they reproduce and reasonably explain the relative capacity of the models for the extra stabilization. We suggest that the overestimation is mainly caused by the error in simulating the electron density on the O atoms. According to the results for similar complexes,[10] a quantitative description of the Coulombic interactions involving OH groups requires a more sophisticated modeling of the electron density on oxygen by centering two more charges on the "lone pair" sites.[10]

To summarize, our ab initio calculations and electrostatic energy analysis suggest that H_2O and CH_3OH adsorb on silica hydroxyls by the 2-fold H-bonding mechanism, forming the extra H-bond to the O atom of the SiOSi or SiOH (in the case of the coordination on geminal OH groups) nearby site.

2. Frequency Analysis. *2.1 Frequency Shifts: Basis Set, Electron Correlation, and Model Size Effects*. Although errors in the computed HF force fields are not insignificant, the HF harmonic frequency approximation correctly describes the intramolecular frequency shifts upon interaction,[25,26,34,35] as for the same fragment in different chemical environments these errors are quantitatively systematic.[39] To illustrate this fact for the involved frequencies, in Table 6 we compare the experimental $\Delta\nu(CH_3)$, $\Delta\nu(OH)$, and $\Delta\delta(OH)$ frequency shifts of CH_3OH linear dimer in matrix isolation[31,40,41] and of CH_3OCH_3 on the silica and zeolitic OH groups[18] with the corresponding HF harmonic frequency shifts of the CH_3OH dimer (**8a**) and of the CH_3OCH_3·$Si(OH)_4$ (**8b**) and CH_3OCH_3·$(HO)_3SiOHAl(OH)_3$ (**8c**) models (Figure 5). The calculations were performed with a combined basis set (CBS2): the 6-311++G(d,p) basis set for the methanol OH group, the dimethyl ether oxygen, and the interacting OH groups of the $Si(OH)_4$ and $(HO)_3SiOHAl(OH)_3$ and the 6-31G(d) basis set for the rest of the complexes. The deviation between the computed and experimental $\Delta\nu(CH_3)$, $\Delta\nu(OH)$, and $\Delta\delta(OH)$ shifts are 3 (average), 2, and 5 cm^{-1}, respectively (Table 6). Considering the possible frequency shifts

TABLE 6: Calculated and Experimental Frequency Shifts (cm^{-1})

model		CBS2[a]	CBS3[a]	6-311++ G(d,p)[b]	MP2/ CBS2[c]	exptl[d]
8a(1)	$\Delta\nu'_{as}(CH_3)$	−19		−19	−20	−13[f]
	$\Delta\nu_s(CH_3)$	−14		−13	−16	−15[f]
	$\Delta\nu(OH)$	(−74)[e]		(−72)[e]	(−108)[e]	−180[g]
	$\Delta\delta(OH)$	(65)[e]		(64)[e]	(88)[e]	49[h]
8a(2)	$\Delta\nu'_{as}(CH_3)$	9		12	5	?
	$\Delta\nu_s(CH_3)$	15		16	15	?
	$\Delta\nu(OH)$	−1		−1	3	−3[g]
	$\Delta\delta(OH)$	3		3	−2	−2[h]
8b[**8b′**]	$\Delta\nu'_{as}(CH_3)$	11	11[9]			9[i]
	$\Delta\nu_s(CH_3)$	17	16[12]			11[i]
8c	$\Delta\nu'_{as}(CH_3)$	25				23[i]
	$\Delta\nu_s(CH_3)$	26				24[i]
8d[**8d′**]	$\Delta\nu(CO)$		18[14]			14[j]

[a] With respect to free CH_3OH $\nu'_{as}(CH_3)$ = 3311 cm^{-1}, $\nu_s(CH_3)$ = 3192 cm^{-1}, $\nu(OH)$ = 4190 cm^{-1}, and $\delta(OH)$ = 1480 cm^{-1}, free CH_3OCH_3 $\nu'_{as}(CH_3)$ = 3306 cm^{-1} and $\nu_s(CH_3)$ = 3181 cm^{-1}, and free CO $\nu(CO)$ = 2432 cm^{-1} frequencies. [b] With respect to free CH_3OH $\nu'_{as}(CH_3)$ = 3261 cm^{-1}, $\nu_s(CH_3)$ = 3147 cm^{-1}, $\nu(OH)$ = 4191 cm^{-1}, and $\delta(OH)$ = 1472 cm^{-1} frequencies. [c] With respect to free CH_3OH $\nu'_{as}(CH_3)$ = 3231 cm^{-1}, $\nu_s(CH_3)$ = 3090 cm^{-1}, $\nu(OH)$ = 3917 cm^{-1}, and $\delta(OH)$ = 1384 cm^{-1} frequencies. [d] With respect to free CH_3OH $\nu'_{as}(CH_3)$ = 3005 cm^{-1}, $\nu_s(CH_3)$ = 2848 cm^{-1}, $\nu(OH)$ = 3667 cm^{-1}, and $\delta(OH)$ = 1348 cm^{-1}. [e] Used for qualitative analysis only (see text). [f] Reference 31. [g] Reference 41. [h] Reference 40. [i] Reference 18. [j] Reference 43.

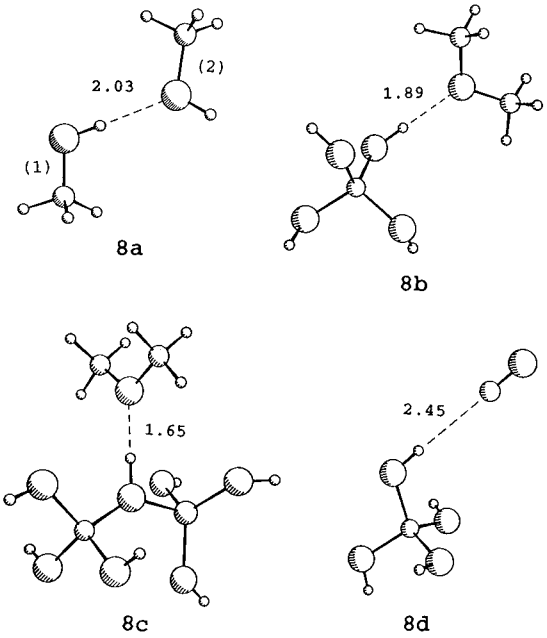

Figure 5. Methanol dimer, molecular models of dimethyl ether on silica and zeolitic OH groups, and molecular model of carbon monoxide on the silica OH group. H-bond lengths in angstroms at the MP2/6-31G(d) level.

TABLE 7: Frequencies of 2-fold Hydrogen-Bonded $CH_3OH{\cdot}Si(OH)_4$ Complexes Computed with Full Geometry Optimized (7a) and under the C_s Symmetry Constraint (5a) (cm^{-1})

	SCF/6-31G(d)		MP2/6-31G(d)	
	7a	**5a**	**7a**	**5a**
$\nu'_{as}(CH_3)$	3310	3310	3226	3228
$\nu_s(CH_3)$	3198	3197	3093	3089
$\nu(OH)^a$	(4059)	(4078)	(3667)	(3721)
$\delta(OH)^a$	(1538)	(1531)	(1465)	(1451)

[a] Used for qualitative analysis only (see text).

of a few cm^{-1} due to the matrix isolation[42] and the accuracy of the experimental measurements of a few cm^{-1}, we regard this agreement between the theoretical and experimental data as a very good one.

To check the basis set and electron correlation effects on the calculated shifts, the CH_3OH dimer was recomputed at the SCF/6-311++G(d,p) and MP2/CBS2 levels; neither the extension of the basis set (cf. CBS2 and 6-311++G(d,p)) nor the inclusion of the electron correlation (cf. CBS2 and MP2/CBS2) affect significantly the results (Table 6). Therefore we suggest the CBS2 shifts to correspond to the theoretical limit of the harmonic approximation within a few cm^{-1}.

$CH_3OCH_3{\cdot}Si(OH)_4$ (**8b**) was calculated also with a smaller combined basis set (CBS3): CBS2 basis set for the adsorbed molecule and the interacting SiOH fragment and the 3-21G basis set for the rest of the complex. This simplification of the description nearly does not change the computed shifts (Table 6). Therefore, to lower the computational cost, we calculated extended models of CH_3OCH_3 and CH_3OH on the OSiOH site with the CBS3 basis set (see below).

To check the model size effect on the calculated shifts, we recomputed CH_3OCH_3 on the silica OH group (**8b**) with the $CH_3OCH_3{\cdot}HOSi(OX)_3$ (X = $Si(OH)_3$) model (**8b′**). This inclusion of the second coordination sphere of silicon atoms with respect to the interacting OH group improves the results: the overestimation of the experimental $\Delta\nu'_{as}(CH_3)$ and $\Delta\nu_s(CH_3)$ shifts by 2 and 5 cm^{-1} decreases to 0 and 1 cm^{-1}, respectively (Table 6). Also in describing CO on the silica OH group such extension of the model causes a similar effect: the overestimation of the $\Delta\nu(CO) = 14$ cm^{-1} shift[43] by 4 cm^{-1} decreases to 0 cm^{-1} on going from the $CO{\cdot}Si(OH)_4$ (**8d**) to $CO{\cdot}HOSi(OX)_3$ (X = $Si(OH)_3$) model (**8d′**) (Table 6). According to the linear dependence of the frequency shifts of probe molecules on the adsorption interaction strength,[44−46] these results suggest that the $Si(OH)_4$ model of the isolated OH group somewhat overestimates the interaction strength, while the extended $HOSi(OX)_3$ (X = $Si(OH)_3$) model provides a better description. Therefore, when calculating the frequency shifts of CH_3OH on the isolated OH group (see below), we used the extended $CH_3OH{\cdot}HOSi(OX)_2OSi(OX)_3$ (**3a′**) and $CH_3OH{\cdot}HOSi(OX)_3$ (**3b′**) (X = $Si(OH)_3$) models for the closed and open structures, respectively, containing the second coordination spheres of silicon atoms with respectm to the OH and O interacting sites of the surface.

In Table 7 we report the $\nu(CH_3)$, $\nu(OH)$, and $\delta(OH)$ frequencies of the 2-fold hydrogen-bonded $CH_3OH{\cdot}Si(OH)_4$ complex computed with full geometry optimization (**7a**) and under the C_s symmetry constraint (**5a**). The symmetry constraint insignificantly influences the $\nu(CH_3)$ frequencies and does not change strongly the $\nu(OH)$ and $\delta(OH)$ frequencies. This result justifies the C_s symmetry imposition for reducing the computational cost in our calculations.

2.2 Frequency Shifts: Dependence on the Adsorption Mechanism. The calculated and experimental data presented in Table 6 allow the derivation of some important qualitative dependencies of the frequency shifts on the hydrogen-bonding mechanism. First, as shown in refs 11 and 12, a hydrogen bond which causes a decrease of the electron charge on the CH_3 group (**8a**(2), **8b**, and **8c**) leads to an increase of the $\nu'_{as}(CH_3)$ and $\nu_s(CH_3)$ frequencies and vice versa (**8a**(1)). Second, while the $\nu(OH)$ and $\delta(OH)$ frequencies of the proton donor CH_3OH (**8a**(1)) are known to shift noticeably to lower and higher frequencies, respectively,[31,40,41,47] those of the proton acceptor CH_3OH (**8a**(2)) are nearly insensitive to the hydrogen bonding. (This was noticed also in a theoretical study by Ugliengo et al.[10]) These data together with the experimental IR data on CH_3OH in NaZSM-5 and KZSM-5 zeolites[48,49] and our results on the simplified $CH_3OH{\cdot}[NaOH{\cdot}2H_2O]$ model (**9**, Figure 6) of CH_3OH in NaZSM-5 zeolite (Table 8) allow one to state that a coordination of CH_3OH through the oxygen should only slightly influence the $\delta(OH)$ vibration in the general case, the $\delta(OH)$ band being very sharp and falling in the narrow 1345−1360 cm^{-1} spectral region (cf. IR spectra in refs 48 and 49, for example).

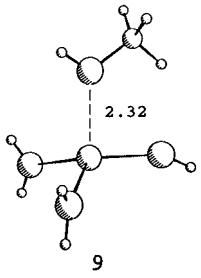

9

Figure 6. Molecular model of methanol on the Na^+ site of zeolites. Bond length in angstroms at the SCF/CBS2 level.

TABLE 8: $\Delta\delta$(OH) Shift of Methanol Interacting through the Oxygen (cm^{-1})

	$\Delta\delta(OH)$
CH_3OH in NaZSM-5 zeolite	9[a]
CH_3OH in KZSM-5 zeolite	3[b]
8a(2)	3[c]
9	3[c]

[a] Reference 48. [b] Reference 49. [c] CBS2.

According to these dependencies, one should expect that if CH_3OH interacts with the isolated silica OH group as a proton acceptor, as proposed by Ugliengo et al.[8,10], then upon CH_3OH adsorption on hydroxylated silica

(a) the $\nu'_{as}(CH_3)$ and $\nu_s(CH_3)$ bands should shift to higher frequencies;

(b) the very sharp band of the $\delta(OH)$ mode should appear in the 1345−1360 cm^{-1} region.

However, as follows from experimental IR data (see below), this is not the case.

2.3 Analysis of Experimental IR Data. The $\Delta\nu(CH_3)$, $\Delta\nu(OH)$, and $\Delta\delta(OH)$ shifts of methanol on the silica OH groups are of prime importance for our determination of the adsorption mechanism. Therefore our assignment of the related experimental frequencies deserves a separate comment. As suggested in ref 17, the first methanol doses admitted on silicalite and silica outgassed at $T \geq 800$ K react with the edge-shared tetrahedral defects (structure **12**)

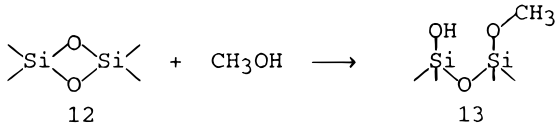

12 13

and with the strained siloxane bridges (structure **14**)

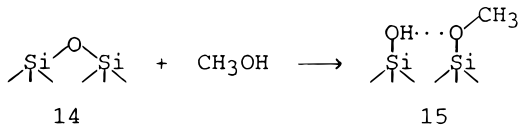

14 15

producing isolated (structure **13**) and hydrogen-bonded (structure **15**) $SiOCH_3$ methoxy groups. The isolated $SiOCH_3$ group manifests itself by $\nu'_{as}(CH_3) = 2997$ cm^{-1}, $\nu''_{as}(CH_3) = 2959$ cm^{-1}, and $\nu_s(CH_3) = 2857$ cm^{-1} bands[15,17,18,32,48] (Figure 7). We first assigned the CH stretching frequencies to the hydrogen-bonded $SiOCH_3$ group:[17] from IR data and calculation results we inferred that the $\nu'_{as}(CH_3)$, $\nu''_{as}(CH_3)$, and $\nu_s(CH_3)$ bands of this species should be shifted by ~20 cm^{-1} to higher frequencies with respect to the corresponding 2997, 2959, and 2857 cm^{-1} bands of the isolated $SiOCH_3$ groups; they should also be broadened due to the structural inhomogeneity of this species. The electron mechanism of these shifts is analogous to that of the upward $\Delta\nu'_{as}(CH_3)$ and $\Delta\nu_s(CH_3)$ shifts of the proton acceptor CH_3OH and CH_3OCH_3 molecules (see above). Only the broad $\nu'_{as}(CH_3) \cong 3020$ cm^{-1} band of this species is observable as a high-frequency shoulder of the 2997 cm^{-1} band,[17] while the $\nu''_{as}(CH_3)$ and $\nu_s(CH_3)$ bands, expected at ~2980 and ~2880 cm^{-1}, cannot be distinguished among other sharp bands in the complex 3000−2860 cm^{-1} spectral region. When the very active edge-shared defects and strained siloxane bridges are used upon successive increase of the coverage, the adsorption takes place on the OH groups. As Sneh and George showed,[50] at this stage CH_3OH initially forms 1:1 hydrogen-bonded complexes with the silica hydroxyls. This CH_3OH species gives rise to the $\nu_s(CH_3)$ band at 2845 cm^{-1} and causes downward shifts of the $\nu'_{as}(CH_3) = 2997$ cm^{-1} and $\nu''_{as}(CH_3) = 2959$ cm^{-} bands by 3 and 9 cm^{-1}, respectively (Figure 7). The appearance of the $\nu_s(CH_3) = 2845$ cm^{-1} band is accompanied by the appearance of a sharp band at 3632 cm^{-1} and a broad band at 1390 cm^{-1} (Figures 7 and 8). We assign them to the ν(OH) and δ(OH) modes of the hydrogen-bonded species, respectively. The 2845 and 3632 cm^{-1} bands were also detected in very thorough IR investigations of the CH_3OH adsorption on silica by Borello et al.[15,16] and attributed to the $\nu_s(CH_3)$ and ν(OH) vibrations of methanol on the OH groups. The changes of the spectra upon the progressive desorption (Figures 7 and 8), which removes the hydrogen-bonded species, supports this assignment of IR bands to CH_3OH on silica OH groups.

Three important conclusions follow from these experimental data on the basis of the above-mentioned dependencies of the frequency shifts on the adsorption mechanism:

1. No sharp δ(OH) band appears in the 1345−1360 cm^{-1} region upon the adsorption (Figure 8). This fact disagrees with the suggestion by Ugliengo et al.[8,10] that CH_3OH stabilizes on the isolated OH group through the oxygen only, i.e. that the hydrogen of the methanol OH group remains nonbonded and its in-plane COH bending vibration is unperturbed.

(2) Also the $\Delta\nu'_{as}(CH_3) = -11$ cm^{-1}, $\Delta\nu_s(CH_3) = -3$ cm^{-1}, and $\Delta\nu$(OH) = −35 cm^{-1} shifts of the CH_3OH with respect to the free methanol $\nu'_{as}(CH_3) = 3005$ cm^{-1}, $\nu_s(CH_3) = 2848$ cm^{-1}, and ν(OH) = 3667 cm^{-1} frequencies[31,40] are at variance with the assumption of the CH_3OH 1-fold hydrogen bonding as a proton acceptor. The $\nu'_{as}(CH_3)$ and $\nu_s(CH_3)$ bands of a proton acceptor CH_3OH should undergo upward, not downward, shifts. As to the ν(OH) frequency, according to Ugliengo et al.[10] and our results (see above), in this mechanism it should change by a few cm^{-1} only.

(3) The following features of the $\Delta\nu$(OH) and $\Delta\delta$(OH) frequency shifts suggest the 2-fold hydrogen bonding of CH_3OH on the OSiOH site:

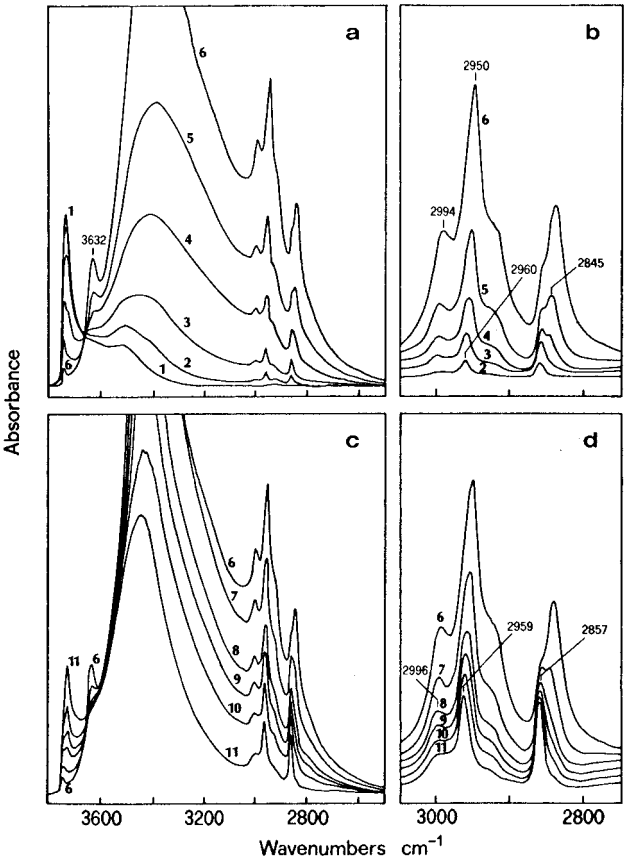

Figure 7. IR spectra of methanol on silicalite (from ref 17). (a) Spectrum 1: silicalite outgassed at 773 K. Spectra 2−6: increasing number of doses up to CH_3OH pressure (2), 50, (3) 10^2, (4) 5×10^2, (5) 10^3, and (6) 2×10^3 Pa. (b) Extended view of the CH stretching region of (a) (after background and hydrogen-bond band tail subtraction). (c) Effect of outgassing. Spectrum 6 corresponds to spectrum 6 of (a). Spectra 7−11: effect of decreasing CH_3OH pressure to (7) 5×10^2, (8) 10^2, (9) 50, (10) 20, and (11) 5 Pa. (d) Extended view of the CH stretching region of (c) (after background and hydrogen-bond band tail subtraction).

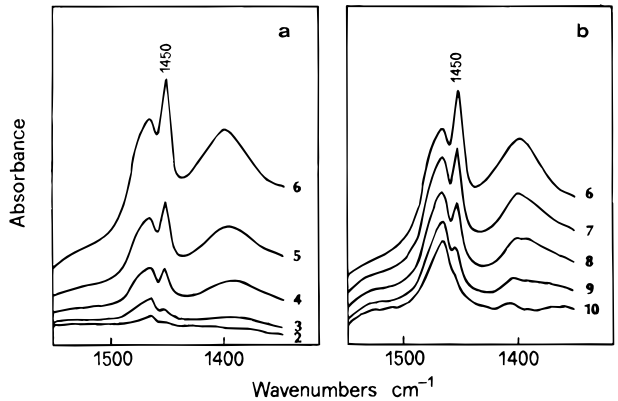

Figure 8. IR spectra of the CH stretching region (from ref 17). (a) Increasing number of CH_3OH doses. Spectra 2−6 correspond to spectra 2−6 of Figure 7. (b) Effect of outgassing. Spectra 6−10 correspond to spectra 6−10 of Figure 7.

(a) according to experimental IR data,[31,40,47] the upward $\Delta\delta$-(OH) = 42 cm^{-1} shift is an indication of the interaction of CH_3-OH as a proton donor. At the same time both IR data[15−17] and energy calculation results[8,10−12,17] suggest the silica hydroxyls to be involved in the interaction as a proton donor too. To explain this fact one should assume that the CH_3OH acts simultaneously as a proton acceptor toward the SiOH group

TABLE 9: MP2/6-311++G $\Delta\nu$(OH) Shift of DOH in Optimal and Strained DOH·OD_2 Dimers[a] (cm^{-1})**

	∠OH···O	$\Delta\nu$(OH)	$\Delta\delta$(OH)
10a	183°	−117	60
10b	150°	−74	55
	140°	−44	45
	130°	−28	39

[a] With respect to free DOH ν(OH) = 3947 cm^{-1} and δ(DOH) = 1427 cm^{-1} frequencies.

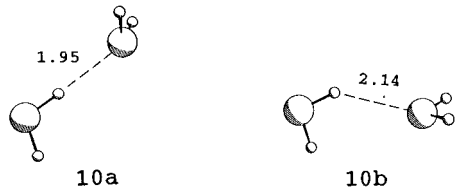

Figure 9. Optimized and strained DOH···OD_2 dimers computed at the MP2/6-311++G(d,p) level. O−H···O angle of strained dimer is 140°. H-bond lengths are in angstroms.

TABLE 10: Frequency Shifts of CH_3OH on the OSiOH Site[a] (cm^{-1})

model	$\Delta\nu'_{as}(CH_3)$	$\Delta\nu_s(CH_3)$	$\Delta\nu$(OH)	$\Delta\delta$(OH)
3a′[b]	−16	1	(−75)[e]	(53)[e]
3b′[b]	5	12	3	−3
exptl[c,d]	−11	−3	−35	32

[a] CBS3 basis set (6-311+G(d,p) basis set for oxygen participating in extra H-bond in **3a′**). [b] With respect to free CH_3OH $\nu'_{as}(CH_3)$ = 3311 cm^{-1}, $\nu_s(CH_3)$ = 3192 cm^{-1}, ν(OH) = 4190 cm^{-1}, and δ(OH) = 1490 cm^{-1} frequencies. [c] With respect to free CH_3OH $\nu'_{as}(CH_3)$ = 3005 cm^{-1}, $\nu_s(CH_3)$ = 2848 cm^{-1}, ν(OH) = 3667 cm^{-1}, and δ(OH) = 1348 cm^{-1} frequencies. [d] Reference 17. [e] Used for qualitative analysis only (see text).

and as a proton donor toward a nearby oxygen of the surface, i.e. by the 2-fold hydrogen-bonding mechanism;[11,12,17]

(b) although the $\Delta\delta$(OH) = 42 cm^{-1} is comparable with the $\Delta\delta$(OH) shifts of methanol upon hydrogen bonding of moderate strength,[31,40,47] the $\Delta\nu$(OH) = −35 cm^{-1} is too small to be accounted for by the formation of an ordinary moderate hydrogen bond. The fact that $|\Delta\nu(OH)|/|\Delta\delta(OH)| < 1$, while usually $|\Delta\nu(OH)|/|\Delta\delta(OH)| \geq 2$,[47] can be accounted for by the 2-fold hydrogen bonding, i.e. by the formation of a strained cyclic structure. As an example, in Table 9 we report the calculated MP2/6-311++G(d,p) $\Delta\nu$(OH) and $\Delta\delta$(OH) shifts of the proton donor DOH molecule in optimal and strained DOH·-OD_2 water dimers (**10a** and **10b**): the O−H···O angles of the three calculated strained dimers were fixed at 150°, 140°, and 130° during the optimization. (The deuterated molecules were used to exclude the coupling effect between the O−H oscillators.) The deviation of the O−H···O angle from the optimum value by more than ∼40° (the corresponding deviation for the MP2/6-31G(d) **3a** model is 47°) leads to the unusual $|\Delta\nu(OH)|/|\Delta\delta(OH)| < 1$ ratio. We suggest that in comparison with the optimal structure in the strained one the OH stretching/bending vibration of the proton donor OH group is accompanied by the smaller/larger change of the hydrogen bond length (Figure 9), which weakens/strengthens the hydrogen-bonding effect on the corresponding frequency.

The computed frequency shifts of the **3a′** and **3b′** extended models of the closed and open CH_3OH structures (Table 10) reinforce this qualitative analysis. The predicted frequency shifts of the open structure conflict with the experimental IR data: the calculations suggest very small $\Delta\nu$(OH) and $\Delta\delta$(OH) shifts to higher and lower frequencies, while significant, opposite shifts to lower and higher frequencies are observed.[15−18] Moreover, the predicted $\Delta\nu'_{as}(CH_3)$ = 5 cm^{-1} and $\Delta\nu_s(CH_3)$ = 12 cm^{-1} shifts contradict the experimental shifts of the $\nu'_{as}(CH_3)$ and $\nu_s(CH_3)$ bands to lower frequencies.[15−18] Unlike the **3b′** model, the **3a′** model of the closed CH_3OH structure shows very good quantitative agreement with the experimental $\Delta\nu'_{as}(CH_3)$ and $\Delta\nu_s(CH_3)$ shifts and qualitative agreement with the experimental Δv(OH) and $\Delta\delta$(OH) shifts.

Conclusion

Two conflicting theoretical interpretations of the adsorption of water and methanol on silica hydroxyls have been proposed by us[9,11,12,17] and by other authors.[1−8,10] The contradiction emerged due to the choice of different molecular models and ab initio approximations, and also due to the fact that in our studies we sought an adsorption mechanism which can satisfy results of both energy calculations and frequency analysis, while in refs 1−8 and 10 the most informative experimental IR data on the involved interaction were ignored. In order to resolve the problem, we have revised our previous conclusions[9,11,12,17] and those of refs 1−8 and 10 using more sophisticated theoretical approaches.

The energy calculations of molecular models suggest that both H_2O and CH_3OH stabilize on the isolated silica OH group by means of two hydrogen bonds: the adsorbing molecules act as a proton acceptor toward the silica OH group and as a proton donor toward a nearby SiOSi bridge of the surface. The calculations predict these adsorption species to be more stable by ∼8 kJ/mol than the 1-fold hydrogen-bonded H_2O and CH_3-OH structures proposed in refs 1−8 and 10, with the adsorbed molecules acting toward the OH group exclusively as a proton acceptor. When stabilizing on the geminal silica OH groups, H_2O and CH_3OH can form the extra hydrogen bond not only with the nearby SiOSi bridge but also with the nearby OH group.

The analysis of the experimental frequency shifts of CH_3OH upon the adsorption reinforces the energy calculation results: the 1-fold hydrogen-bonded CH_3OH species disagree with the observed $\Delta\nu(CH_3)$, $\Delta\nu$(OH), and $\Delta\delta$(OH) shifts of methanol on silica hydroxyls, while the 2-fold hydrogen-bonded species is in good agreement with the experimental IR data.

The checks of basis set, electron correlation, and model size effects on the computed adsorption energies and frequencies support the reliability of our results. The analysis of the electrostatic interactions in the H_2O·$HOSiH_2OSiH_3$ model used in ref 8 suggests that this model is not adequate for studying the mechanism in question. The inadequacy mainly results from a significant underestimation of the q(Si) charge of the Si atom bonded to the adsorbing OH group, due to the not realistic chemical coordination of this Si atom in the model compared with its pure oxygen surroundings in silica. Considering the prevailing role of the Coulombic interactions in the moderate strength H-bonding, the use of such models for examining small differences in binding energy between hypothetical adsorption mechanisms is doubtful.

Acknowledgment. We are grateful to both the Italian CNR and MURST for financial support of this research. A.G.P. gratefully acknowledges the Italian CNR for a NATO Guest fellowship. We also thank Prof. Adriano Zecchina and Dr. Silvia Bordiga for very useful discussion of our calculation results.

References and Notes

(1) Hobza, P.; Sauer, J.; Morgeneyer, C.; Hurych, J.; Zahradnik, R. *J. Phys. Chem.* **1981**, *85*, 4061.
(2) Sauer, J.; Zahradnik, R. *Int. J. Quantum Chem.* **1984**, *26*, 793.
(3) Sauer, J.; Schroder, K.-P. *Chem. Phys. Lett.* **1984**, *107*, 530.
(4) Sauer, J.; Schroder, K.-P. *Z. Phys. Chem. (Leipzig)* **1985**, *266*, 379.

(5) Zhidomirov, G. M.; Kazansky, V. B. *Adv. Catal*. **1986**, *34*, 131.
(6) Chakoumakos, B. C.; Gibbs, G. V. *J. Phys. Chem*. **1986**, *90*, 996.
(7) Ugliengo, P.; Saunders, V. R.; Garrone, E. *J. Phys. Chem*. **1990**, *94*, 2260.
(8) Sauer, J.; Ugliengo, P.; Garrone, E.; Saunders, V. R. *Chem. Rev*. **1994**, *94*, 2095.
(9) Pelmenschikov, A. G.; Morosi, G.; Gamba, A. *J. Phys. Chem*. **1992**, *96*, 7422.
(10) Ugliengo, P.; Bleiber, A.; Garrone, E.; Sauer, J.; Ferrari, A. M. *Chem. Phys. Lett*. **1992**, *191*, 537.
(11) Pelmenschikov, A. G.; Morosi, G.; Gamba, A. *J. Phys. Chem*. **1992**, *96*, 2241.
(12) Pelmenschikov, A. G.; Morosi, G.; Gamba, A. In *Proceedings of the 9th International Zeolite Conference*, Montreal 1992; von Ballmoos, R., Higgins, J. B., Treacy, M. M. J., Eds.; Butterworth-Heinemann: London, 1993; p 537.
(13) Gutmann, V. *The Donor-Acceptor Approach to Molecular Interactions*; Plenum Press: New York, 1978.
(14) Chung, J. S.; Bennett, C. O. *J. Catal*. **1985**, *92*, 173.
(15) Borello, E.; Zecchina, A.; Morterra, C. *J. Phys. Chem*. **1967**, *71*, 2938.
(16) Borello, E.; Zecchina, A.; Morterra, C.; Ghiotti, G. *J. Phys. Chem*. **1967**, *71*, 2945.
(17) Pelmenschikov, A. G.; Morosi, G.; Gamba, A.; Zecchina, A.; Bordiga, S.; Paukshtis, E. A. *J. Phys. Chem*. **1993**, *97*, 11979.
(18) Forester, T. R.; Howe, R. F. *J. Am. Chem. Soc*. **1987**, *109*, 5076.
(19) Walrefen, G. E.; Luck, W. A. P. In *Structure of water and aqueous solutions*; Luck, W. A. P., Ed.; Verlag Chemie: Weinham, 1974; p 222.
(20) Shivaglal, M. C.; Sing, S. *Int. J. Quantum Chem*. **1989**, *36*, 105.
(21) Brakaspathy, R.; Sing, S. *Chem. Phys. Lett*. **1986**, *131*, 394.
(22) Maes, G.; Smets, J. *J. Phys. Chem*. **1993**, *97*, 1818.
(23) Ugliengo, P.; Ferrari, A. M.; Zecchina, A.; Garrone, E. *J. Phys. Chem*. **1996**, *100*, 3632.
(24) Ferrari, A. M.; Ugliengo, P.; Garrone, E. *J. Phys. Chem*. **1993**, *97*, 2671.
(25) Pelmenschikov, A. G.; Morosi, G.; Gamba, A.; Coluccia, S. *J. Phys. Chem*. **1995**, *99*, 15018.
(26) Pelmenschikov, A. G.; Morosi, G.; Gamba, A.; Coluccia, S.; Martra, G.; Paukshtis, E. A. *J. Phys. Chem*. **1996**, *100*, 5011.
(27) Frisch, M. J.; Trucks, G. W.; Head-Gordon, M.; Gill, P. M. W.; Wong, M. W.; Foresman, J. B.; Johnson, B. G.; Schlegel, H. B.; Robb, M. A.; Replogle, E. S.; Gomperts, R.; Andres, J. L.; Raghavachari, K.; Binkley, J. S.; Gonzalez, C.; Martin, R. L.; Fox, D. J.; Defrees, D. J.; Baker, J.; Stewart, J. J. P.; Pople, J. A. *GAUSSIAN 92 (Revision A)*; Gaussian, Inc.: Pittsburgh, PA, 1992.
(28) Frisch, M. J.; Trucks, G. W.; Schlegel, H. B.; Gill, P. M. W.; Johnson, B. G.; Robb, M. A.; Cheeseman, J. R.; Keith, G. A.; Petersson, G. A.; Montgomery, J. A.; Raghavachari, K.; Al-Laham, M. A.; Zakrzewski, V. G.; Ortiz, J. V.; Foresman, J. B.; Cioslowski, J.; Stefanov, B. B.; Nanayakkara, A.; Challacombe, M.; Peng, C. Y.; Ayala, P. Y.; Chen, W.; Wong, M. W.; Andres, J. L.; Replogle, E. S.; Gomperts, R.; Martin, R. L.; Fox, D. J.; Binkley, J. S.; Defrees, D. J.; Baker, J.; Stewart, J. P.; Head-Gordon, M.; Gonzalez, C.; Pople, J. A. *GAUSSIAN 94 (Revision A.1)*; Gaussian, Inc.: Pittsburgh, PA, 1995.
(29) Boys, S. F.; Bernardi, F. *Mol. Phys*. **1970**, *19*, 553.
(30) Breneman, C. M.; Wiberg, K. B. *J. Comput. Chem*. **1990**, *11*, 361.
(31) Barnes, A. J.; Hallam, H. E. *Trans. Faraday Soc*. **1970**, *66*, 1920.
(32) Morrow, B. A. *J. Chem. Soc., Faraday Trans. 1* **1974**, *70*, 1527.
(33) Bleiber, A.; Sauer, J. *Chem. Phys. Lett*. **1995**, *238*, 243.
(34) Scheiner, S. In *Ab Initio Studies of Hydrogen Bonding*, Marksic', Z. B., Ed.; Springer-Verlag: Berlin, 1991; p 173.
(35) Hehre, W. J.; Radom, L.; Schleyer, P. v.R.; Pople, J. A. *Ab Initio Molecular Orbital Theory*; Wiley-Interscience: New York, 1986.
(36) Becke, A. D. *Phys. Rev*. **1988**, *B38*, 3098.
(37) Lee, C.; Yang, W.; Parr, R. G. *Phys. Rev*. **1988**, *B37*, 785.
(38) We follow the recommendation proposed in ref 33 to consider the normal modes characterized by frequencies less then 500 cm^{-1} and corresponding to the torsion around a single bond as pure rotations. The computed MP2/6-31G(d) frequencies of the H_2O and CH_3OH torsion around the H-bond in models **6b** and **7b** are 115 and 60 cm^{-1}, respectively.
(39) Pulay, P.; Fogarasi, G.; Pongor, G.; Boggs, J. E.; Vargha, A. *J. Am. Chem. Soc*. **1983**, *105*, 7037.
(40) Murto, J.; Räsänen, M.; Aspiala, A.; Kemppinen, E. *Acta Chem. Scand*. **1983**, *A37*, 323.
(41) Luck, W. A. P.; Schrems, O. *J. Mol. Struct*. **1980**, *60*, 333.
(42) Cf. CH_3OH frequencies in argon and nitrogen matrices[39,40] and in the gas phase (Falk, M.; Whalley, E. *J. Chem. Phys*. **1961**, *34*, 1554).
(43) Kustov, L. M.; Kazansky, V. B.; Beran, S.; Kubelkova, L.; Jiru, P. *J. Phys. Chem*. **1987**, *91*, 5247.
(44) Roxhet, P. G.; Sempels, R. E. *J. Chem. Soc., Faraday Trans. 1* **1974**, *70*, 2021.
(45) Bohem, H.-P.; Knozinger, H. In *Catalysis Science and Technology*; Anderson, J. R., Boudart, M., Eds.; Springer: Berlin, 1983; Vol. 4, p 39.
(46) Zaki, M. I.; Knozinger, H. *Mater. Chem. Phys*. **1987**, *17*, 201.
(47) Pimentel, G. C.; McClellan, A. L. *The Hydrogen Bond*; Reinold Publishing Corp.: New York, 1960.
(48) Kubelkova, L.; Novakova, J.; Nedomova, K. *J. Catal*. **1990**, *124*, 441.
(49) Mirth, G.; Lercher, J. A.; Anderson, M. W.; Klinowsky, J. *J. Chem. Soc., Faraday Trans*. **1990**, *86* (17), 3039.
(50) Sneh, O.; George, S. M. *J. Phys. Chem*. **1995**, *99*, 4639.